View metadata, citation and similar papers at core.ac.uk

brought to you by CORE

provided by CiteSeerX

Energy Conversion and Management 50 (2009) 2554–2561

Contents lists available at ScienceDirect

Energy Conversion and Management

journal homepage: www.elsevier.com/locate/enconman

Design of output feedback UPFC controller for damping of electromechanical oscillations using PSO

H. Shayeghi [a,*], H.A. Shayanfar [b], S. Jalilzadeh [c], A. Safari [c]

[a] Technical Engineering Department, University of Mohaghegh Ardabili, Ardabil, Iran
[b] Center of Excellence for Power Automation and Operation, Electrical Engineering Department, Iran University of Science and Technology, Tehran, Iran
[c] Technical Engineering Department, Zanjan University, Zanjan, Iran

ARTICLE INFO

Article history:
Received 4 November 2008
Accepted 8 June 2009
Available online 7 July 2009

Keywords:
UPFC
Output feedback
PSO
Dynamic stability
Power system oscillations

ABSTRACT

In this paper, a novel method for the design of output feedback controller for unified power flow controller (UPFC) is developed. The selection of the output feedback gains for the UPFC controllers is converted to an optimization problem with the time domain-based objective function which is solved by a particle swarm optimization technique (PSO) that has a strong ability to find the most optimistic results. Only local and available state variables are adopted as the input signals of each controller for the decentralized design. Thus, structure of the designed UPFC controller is simple and easy to implement. To ensure the robustness of the proposed stabilizers, the design process takes into account a wide range of operating conditions and system configurations. The effectiveness of the proposed controller for damping low frequency oscillations is tested and demonstrated through nonlinear time-domain simulation and some performance indices studies. The results analysis reveals that the designed PSO-based output feedback UPFC damping controller has an excellent capability in damping power system low frequency oscillations and enhance greatly the dynamic stability of the power systems. Moreover, the system performance analysis under different operating conditions show that the δ_E based controller is superior to both the m_B based controller and conventional power system stablizer.

© 2009 Elsevier Ltd. All rights reserved.

1. Introduction

As power demand grows rapidly and expansion in transmission and generation is restricted with the limited availability of resources and the strict environmental constraints, power systems are today much more loaded than before. This causes the power systems to be operated near their stability limits. In addition, interconnection between remotely located power systems gives rise to low frequency oscillations in the range of 0.2–3.0 Hz. If not well damped, these oscillations may keep growing in magnitude until loss of synchronism results [1,2]. In order to damp these power system oscillations and increase system oscillations stability, the installation of power system stabilizer (PSS) is both economical and effective. PSSs have been used for many years to add damping to electromechanical oscillations. However, PSSs suffer a drawback of being liable to cause great variations in the voltage profile and they may even result in leading power factor operation and losing system stability under severe disturbances, especially those three-phase faults which may occur at the generator terminals [3].

In recent years, the fast progress in the field of power electronics had opened new opportunities for the application of the FACTS devices as one of the most effective ways to improve power system operation controllability and power transfer limits [1–4]. Through the modulation of bus voltage, phase shift between buses, and transmission line reactance, FACTS devices can cause a substantial increase in power transfer limits during steady-state. Because of the extremely fast control action associated with FACTS-device operations, they have been very promising candidates for utilization in power system damping enhancement. It has been observed that utilizing a feedback supplementary control, in addition to the FACTS-device primary control, can considerably improve system damping and can also improve system voltage profile, which is advantageous over PSSs.

The unified power flow controller (UPFC) is regarded as one of the most versatile devices in the FACTS-device family [5,6] which has the ability to control of the power flow in the transmission line, improve the transient stability, mitigate system oscillation and provide voltage support. It performs this through the control of the in-phase voltage, quadrate voltage and shunts compensation due to its mains control strategy [1,4]. The application of the UPFC to the modern power system can therefore lead to the more flexible, secure and economic operation [7]. When the UPFC is applied to the interconnected power systems, it can also provide

* Corresponding author. Address: Daneshgah Street, P.O. Box 179, Ardabil, Iran. Tel.: +98 451 5517374; fax: +98 451 5512904.
E-mail address: hshayeghi@gmail.com (H. Shayeghi).

0196-8904/$ - see front matter © 2009 Elsevier Ltd. All rights reserved.
doi:10.1016/j.enconman.2009.06.005

significant damping effect on tie line power oscillation through its supplementary control.

Several trials have been reported in the literature to dynamic models of UPFC in order to design suitable controllers for power flow, voltage and damping controls [8]. Nabavi-Niaki and Iravani [9] developed a steady-state model, a small-signal linearized dynamic model, and a state-space large-signal model of a UPFC. Wang [10–12] presents the establishment of the linearized Phillips–Heffron model of a power system installed with a UPFC. Wang has not presented a systematic approach for designing the damping controllers. Further, no effort seems to have been made to identify the most suitable UPFC control parameter, in order to arrive at a robust damping controller. Wang and Swift [13] developed a novel unified Phillips–Heffron model for a power system equipped with a SVC, a TCSC and a TCPS. Damping torque coefficient analysis has been performed based on the proposed model to study the effect of FACTS controllers damping for different loading conditions. Huang et al. [14] attempted to design a conventional fixed-parameter lead-lag controller for a UPFC installed in the tie line of a two-area system to damp the inter-area mode of oscillations.

An industrial process, such as a power system, contains different kinds of uncertainties due to continuous load changes or parameters drift due to power systems highly nonlinear and stochastic operating nature. Consequently, a fixed-parameter controller based on the classical control theory is not certainly suitable for the UPFC damping control design. Thus, it is required that a flexible controller be developed. Some authors suggested neural networks method [15] and robust control methodologies [7,16] to cope with system uncertainties to enhance the system damping performance using the UPFC. However, the parameters adjustments of these controllers need some trial and error. Also, although using the robust control methods, the uncertainties are directly introduced to the synthesis, but due to the large model order of power systems the order resulting controller will be very large in general, which is not feasible because of the computational economical difficulties in implementing. Some authors used fuzzy logic based damping control strategy for TCSC, UPFC and SVC in a multi-machine power system [17–19]. The damping control strategy employs non-optimal fuzzy logic controllers that is why the system's response settling time is unbearable. Moreover, the initial parameters adjustment of this type of controller needs some trial and error. Khon and Lo [20] used a fuzzy damping controller designed by micro Genetic Algorithm (GA) for TCSC and UPFC to improve powers system low frequency oscillations. The proposed method may have not enough robustness due to its simplicity against the different kinds of uncertainties and disturbances. Mok et al. [21] applied a GA-based Proportional–Integral (PI) type fuzzy controller for UPFC to enhance power system damping. Although, the fuzzy PI controller is simpler and more applicable to remove the steady state error, it is known to give poor performance in the system transient response.

In general, for the simplicity of practical implementation of the controllers, decentralized output feedback control with feedback signals available at the location of the each controlled device is most favorable. Methods for the selection of the TCSC installation locations and the output feedback signals have been developed and reported in [22,23]. In this paper, PSO technique is used for optimal tuning of output feedback gains for the UPFC controllers to improve optimization synthesis and the speed of algorithms convergence. PSO is a novel population based metaheuristic, which utilize the swarm intelligence generated by the cooperation and competition between the particle in a swarm and has emerged as a useful tool for engineering optimization. Unlike the other heuristic techniques, it has a flexible and well-balanced mechanism to enhance the global and local exploration abilities. Also, it suffices to specify the objective function and to place finite bounds on the optimized parameters.

A new approach for the optimal decentralized design of output feedback gains for the UPFC damping controller is investigated in this paper. A performance index is defined based on the system dynamics after an impulse disturbance alternately occurs in system and it is organized for a wide range of operating conditions and used to form the objective function of the design problem. The problem of robust output feedback controller design is formulated as an optimization problem and PSO technique is used to solve it. The proposed design process for controller with the output feedback scheme is applied to a single-machine infinite-bus power system. Since only local and available states ($\Delta\omega$ and ΔV_t) are used as the inputs of each controller, the optimal decentralized design of controller can be accomplished. The effectiveness of the proposed controller is demonstrated through nonlinear time-domain simulation studies and some performance indices to damp low frequency oscillations under different operating conditions. Results evaluation show that the proposed output feedback UPFC damping controller achieves good robust performance for a wide range of operating conditions and disturbances.

2. PSO technique

Particle swarm optimization algorithm, which is tailored for optimizing difficult numerical functions and based on metaphor of human social interaction, is capable of mimicking the ability of human societies to process knowledge [25]. It has roots in two main component methodologies: artificial life (such as bird flocking, fish schooling and swarming); and, evolutionary computation. Its key concept is that potential solutions are flown through hyperspace and are accelerated towards better or more optimum solutions. Its paradigm can be implemented in simple form of computer codes and is computationally inexpensive in terms of both memory requirements and speed. It lies somewhere in between evolutionary programming and the genetic algorithms. As in evolutionary computation paradigms, the concept of fitness is employed and candidate solutions to the problem are termed particles or sometimes individuals, each of which adjusts its flying based on the flying experiences of both itself and its companion. It keeps track of its coordinates in hyperspace which are associated with its previous best fitness solution, and also of its counterpart corresponding to the overall best value acquired thus far by any other particle in the population. Vectors are taken as presentation of particles since most optimization problems are convenient for such variable presentations. In fact, the fundamental principles of swarm intelligence are adaptability, diverse response, proximity, quality, and stability. It is adaptive corresponding to the change of the best group value. The allocation of responses between the individual and group values ensures a diversity of response. The higher dimensional space calculations of the PSO concept are performed over a series of time steps. The population is responding to the quality factors of the previous best individual values and the previous best group values. The principle of stability is adhered to since the population changes its state if and only if the best group value changes. As it is reported in [26], this optimization technique can be used to solve many of the same kinds of problems as GA, and does not suffer from some of GAs difficulties. It has also been found to be robust in solving problem featuring non-linearity, non-differentiability and high-dimensionality. PSO is the search method to improve the speed of convergence and find the global optimum value of fitness function.

PSO starts with a population of random solutions "particles" in a D-dimension space. The ith particle is represented by $X_i = (x_{i1}, x_{i2}, \ldots, x_{iD})$. Each particle keeps track of its coordinates in hyperspace, which are associated with the fittest solution it has achieved so far. The value of the fitness for particle i ($p$best) is also stored as

$P_i = (p_{i1}, p_{i2}, \ldots, p_{iD})$. The global version of the PSO keeps track of the overall best value (gbest), and its location, obtained thus far by any particle in the population. PSO consists of, at each step, changing the velocity of each particle toward its pbest and gbest according to Eq. (1). The velocity of particle i is represented as $V_i = (v_{i1}, v_{i2}, \ldots, v_{iD})$. Acceleration is weighted by a random term, with separate random numbers being generated for acceleration toward pbest and gbest. The position of the ith particle is then updated according to Eq. (2) [25,26].

$$v_{id} = w \times v_{id} + c_1 \times rand() \times (P_{id} - x_{id}) + c_2 \times rand() \times (P_{gd} - x_{id}) \quad (1)$$

$$x_{id} = x_{id} + c\,v_{id} \quad (2)$$

where P_{id} and P_{gd} are pbest and gbest. Several modifications have been proposed in the literature to improve the PSO algorithm speed and convergence toward the global minimum. One modification is to introduce a local-oriented paradigm (lbest) with different neighborhoods. It is concluded that gbest version performs best in terms of median number of iterations to converge. However, Pbest version with neighborhoods of two is most resistant to local minima. PSO algorithm is further improved via using a time decreasing inertia weight, which leads to a reduction in the number of iterations [24]. Fig. 1 shows the flowchart of the proposed PSO algorithm.

This new approach features many advantages; it is simple, fast and easy to be coded. Also, its memory storage requirement is minimal. Moreover, this approach is advantageous over evolutionary and genetic algorithms in many ways. First, PSO has memory. That is, every particle remembers its best solution (local best) as well as the group best solution (global best). Another advantage of PSO is that the initial population of the PSO is maintained, and so there is no need for applying operators to the population, a process that is time and memory-storage-consuming. In addition, PSO is based on "constructive cooperation" between particles, in contrast with the genetic algorithms, which are based on "the survival of the fittest".

3. Description of case study system

Fig. 2 shows a single-machine infinite-bus (SMIB) power system equipped with a UPFC. The synchronous generator is delivering power to the infinite-bus through a double circuit transmission line and a UPFC. The UPFC consists of an excitation transformer (ET), a boosting transformer (BT), two three-phase GTO based voltage source converters (VSCs), and a DC link capacitors. The four input control signals to the UPFC are m_E, m_B, δ_E, and δ_B, where, m_E is the excitation amplitude modulation ratio, m_B is the boosting amplitude modulation ratio, δ_E is the excitation phase angle and δ_B is the boosting phase angle.

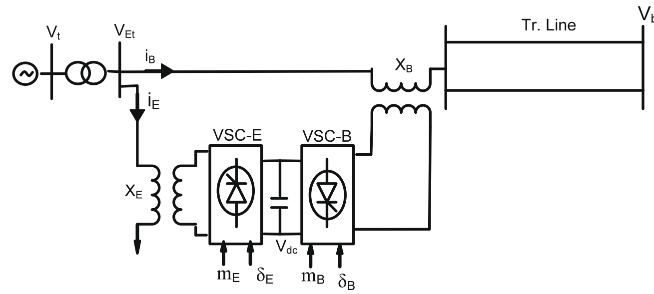

Fig. 2. SMIB power system equipped with UPFC.

3.1. Power system nonlinear model with UPFC

The dynamic model of the UPFC is required in order to study the effect of the UPFC for enhancing the small-signal stability of the power system. The system data is given in the Appendix A. By applying Park's transformation and neglecting the resistance and transients of the ET and BT transformers, the UPFC can be modeled as [10–12]:

$$\begin{bmatrix} v_{Etd} \\ v_{Etq} \end{bmatrix} = \begin{bmatrix} 0 & -x_E \\ x_E & 0 \end{bmatrix} \begin{bmatrix} i_{Ed} \\ i_{Eq} \end{bmatrix} + \begin{bmatrix} \frac{m_E \cos\delta_E v_{dc}}{2} \\ \frac{m_E \sin\delta_E v_{dc}}{2} \end{bmatrix} \quad (3)$$

$$\begin{bmatrix} v_{Btd} \\ v_{Btq} \end{bmatrix} = \begin{bmatrix} 0 & -x_B \\ x_B & 0 \end{bmatrix} \begin{bmatrix} i_{Bd} \\ i_{Bq} \end{bmatrix} + \begin{bmatrix} \frac{m_B \cos\delta_B v_{dc}}{2} \\ \frac{m_B \sin\delta_B v_{dc}}{2} \end{bmatrix} \quad (4)$$

$$\dot{v}_{dc} = \frac{3m_E}{4C_{dc}} [\cos\delta_E \quad \sin\delta_E] \begin{bmatrix} i_{Ed} \\ i_{Eq} \end{bmatrix} + \frac{3m_B}{4C_{dc}} [\cos\delta_B \quad \sin\delta_B] \begin{bmatrix} i_{Bd} \\ i_{Bq} \end{bmatrix} \quad (5)$$

where v_{Et}, i_E, v_{Bt}, and i_B are the excitation voltage, excitation current, boosting voltage, and boosting current, respectively; C_{dc} and v_{dc} are the DC link capacitance and voltage. The nonlinear model of the SMIB system as shown in Fig. 2 is described by [1]:

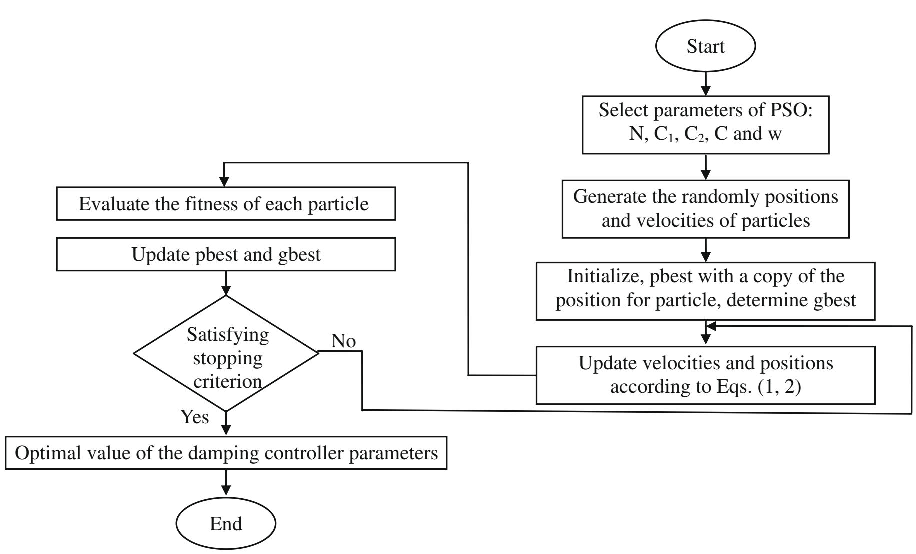

Fig. 1. Flowchart of the proposed PSO technique.

$$\dot{\delta} = \omega_0(\omega - 1) \tag{6}$$
$$\dot{\omega} = (P_m - P_e - D\Delta\omega)/M \tag{7}$$
$$\dot{E}'_q = (-E_q + E_{fd})/T'_{do} \tag{8}$$
$$\dot{E}_{fd} = (-E_{fd} + K_a(V_{ref} - V_t))/T_a \tag{9}$$

where,

$$P_e = V_{td}I_{td} + V_{tq}I_{tq}; \quad E_q = E'_{qe} + (X_d - X'_d)I_{td};$$
$$V_t = V_{td} + jV_{tq}; \quad V_{td} = X_qI_{tq}; \quad V_{tq} = E'_q - X'_dI_{td};$$
$$I_{td} = I_{tld} + I_{Ed} + I_{Bd}; \quad I_{tq} = I_{tlq} + I_{Eq} + I_{Bq}$$

From Fig. 2. we can have:

$$\bar{v}_t = jx_{tE}(\bar{i}_B + \bar{i}_E) + \bar{v}_{Et} \tag{10}$$
$$\bar{v}_{Et} = \bar{v}_{Bt} + jx_{BV}\bar{i}_B + \bar{v}_b \tag{11}$$

$$\begin{aligned} v_{td} + jv_{tq} &= x_q(i_{Eq} + i_{Bq}) + j(E'_q - x'_d(i_{Ed} + i_{Bd})) \\ &= jx_{tE}(i_{Ed} + i_{Bd} + j(i_{Eq} + i_{Bq})) + v_{Etd} + jv_{Etq} \end{aligned} \tag{12}$$

where i_t and v_b, are the armature current and infinite-bus voltage, respectively. From the above equations, we can obtain:

$$\begin{aligned} i_{Ed} &= \frac{x_{BB}}{x_{d\sum}}E'_q - \frac{m_E \sin\delta_E v_{dc} x_{Bd}}{2x_{d\sum}} \\ &\quad + \frac{x_{dE}}{x_{d\sum}}\left(v_b\cos\delta + \frac{m_B\sin\delta_B v_{dc}}{2}\right) \end{aligned} \tag{13}$$

$$i_{Eq} = \frac{m_E\cos\delta_E v_{dc}x_{Bq}}{2x_{q\sum}} - \frac{x_{qE}}{x_{q\sum}}\left(v_b\sin\delta + \frac{m_B\cos\delta_B v_{dc}}{2}\right) \tag{14}$$

$$\begin{aligned} i_{Bd} &= \frac{x_E}{x_{d\sum}}E'_q + \frac{m_E\sin\delta_E v_{dc}x_{dE}}{2x_{d\sum}} \\ &\quad - \frac{x_{dt}}{x_{d\sum}}\left(v_b\cos\delta + \frac{m_B\sin\delta_B v_{dc}}{2}\right) \end{aligned} \tag{15}$$

$$i_{Bq} = -\frac{m_E\cos\delta_E v_{dc}x_{qE}}{2x_{q\sum}} + \frac{x_{qt}}{x_{q\sum}}\left(v_b\sin\delta + \frac{m_B\cos\delta_B v_{dc}}{2}\right) \tag{16}$$

where,

$$x_{q\sum} = (x_q + x_T + x_E)\left(x_B + \frac{x_L}{2}\right) + x_E(x_q + x_T)$$

$$x_{Bq} = x_q + x_T + x_B + \frac{x_L}{2}$$

$$x_{qt} = x_q + x_T + x_E; \quad x_{qE} = x_q + x_T;$$
$$x_{d\sum} = (x'_d + x_T + x_E)\left(x_B + \frac{x_L}{2}\right) + x_E(x'_d + x_T)$$

$$x_{Bd} = x'_d + x_T + x_B + \frac{x_L}{2}; \quad x_{Bd} = x'_d + x_T + x_E; \quad x_{dE} = x'_d + x_T;$$
$$x_{BB} = x_B + \frac{x_L}{2}$$

x_E, x_B, x_d, x'_d and x_q are the ET, BT reactance, d-axis reactance, d-axis transient reactance, and q-axis reactance, respectively.

3.2. Power system linearized model

A linear dynamic model is obtained by linearizing the nonlinear model round an operating condition. The linearized model of power system as shown in Fig. 2 is given as follows:

$$\Delta\dot{\delta} = \omega_0\Delta\omega \tag{17}$$
$$\Delta\dot{\omega} = (-\Delta P_e - D\Delta\omega)/M \tag{18}$$
$$\dot{E}'_q = (-\Delta E_q + \Delta E_{fd})/T'_{do} \tag{19}$$
$$\Delta\dot{E}_{fd} = (K_A(\Delta v_{ref} - \Delta v) - \Delta E_{fd})/T_A \tag{20}$$

$$\begin{aligned} \Delta\dot{v}_{dc} &= K_7\Delta\delta + K_8\Delta E'_q - K_9\Delta v_{dc} + K_{ce}\Delta m_E + K_{c\delta e}\Delta\delta_E \\ &\quad + K_{cb}\Delta m_B + K_{c\delta b}\Delta\delta_B \end{aligned} \tag{21}$$

$$\begin{aligned} \Delta P_e &= K_1\Delta\delta + K_2\Delta E'_q + K_{pd}\Delta v_{dc} + K_{pe}\Delta m_E + K_{p\delta e}\Delta\delta_E \\ &\quad + K_{pb}\Delta m_B + K_{p\delta b}\Delta\delta_B \end{aligned} \tag{22}$$

$$\begin{aligned} \Delta E'_q &= K_4\Delta\delta + K_3\Delta E'_q + K_{qd}\Delta v_{dc} + K_{qe}\Delta m_E + K_{q\delta e}\Delta\delta_E \\ &\quad + K_{qb}\Delta m_B + K_{q\delta b}\Delta\delta_B \end{aligned} \tag{23}$$

$$\begin{aligned} \Delta V_t &= K_5\Delta\delta + K_6\Delta E'_q + K_{vd}\Delta v_{dc} + K_{ve}\Delta m_E + K_{v\delta e}\Delta\delta_E \\ &\quad + K_{vb}\Delta m_B + K_{v\delta b}\Delta\delta_B \end{aligned} \tag{24}$$

$K_1, K_2, \ldots, K_9$, K_{pu}, K_{qu} and K_{vu} are linearization constants. The state-space model of power system is given by:

$$\dot{x} = Ax + Bu \tag{25}$$

where the state vector x, control vector u, A and B are:

$$x = [\Delta\delta \quad \Delta\omega \quad \Delta E'_q \quad \Delta E_{fd} \quad \Delta v_{dc}]; \quad u = [\Delta m_E \quad \Delta\delta_E \quad \Delta m_B \quad \Delta\delta_B]^T$$

$$A = \begin{bmatrix} 0 & w_0 & 0 & 0 & 0 \\ -\frac{K_1}{M} & 0 & -\frac{K_2}{M} & 0 & -\frac{K_{pd}}{M} \\ -\frac{K_4}{T'_{do}} & 0 & -\frac{K_3}{T'_{do}} & \frac{1}{T'_{do}} & -\frac{K_{qd}}{T'_{do}} \\ -\frac{K_AK_5}{T_A} & 0 & -\frac{K_AK_6}{T_A} & -\frac{1}{T_A} & -\frac{K_AK_{vd}}{T_A} \\ K_7 & 0 & K_8 & 0 & -K_9 \end{bmatrix};$$

$$B = \begin{bmatrix} 0 & 0 & 0 & 0 \\ -\frac{K_{pe}}{M} & -\frac{K_{p\delta e}}{M} & -\frac{K_{pb}}{M} & -\frac{K_{p\delta b}}{M} \\ -\frac{K_{qe}}{T'_{do}} & -\frac{K_{q\delta e}}{T'_{do}} & -\frac{K_{qb}}{T'_{do}} & -\frac{K_{q\delta b}}{T'_{do}} \\ -\frac{K_AK_{vc}}{T_A} & -\frac{K_AK_{v\delta e}}{T_A} & -\frac{K_AK_{vb}}{T_A} & -\frac{K_AK_{v\delta b}}{T_A} \\ K_{ce} & K_{c\delta e} & K_{cb} & K_{c\delta b} \end{bmatrix}$$

The block diagram of the linearized dynamic model of the SMIB power system with UPFC is shown in Fig. 3.

3.3. PSO-based output feedback controller design

A power system can be described by a linear time invariant (LTI) state-space model as follows [28]:

$$\begin{aligned} \dot{x} &= Ax + Bu \\ y &= Cx \end{aligned} \tag{26}$$

where x, y and u denote the system linearized state, output and input variable vectors, respectively. A, B and C are constant matrixes with appropriate dimensions which are dependent on the operating point of the system. The eigenvalues of the state matrix A that are called the system modes define the stability of the system when it is affected by a small interruption. As long as all eigenvalues have negative real parts, the power system is stable when it is subjected to a small disturbance. If one of these modes has a positive real part the system is unstable. In this case, using either the output or the state feedback controller can move the unstable mode to the left-hand side of the complex plane in the area of the negative real parts. An output feedback controller has the following structures:

$$u = -Ky \tag{27}$$

Substituting (27) into (26) the resulting state equation is:

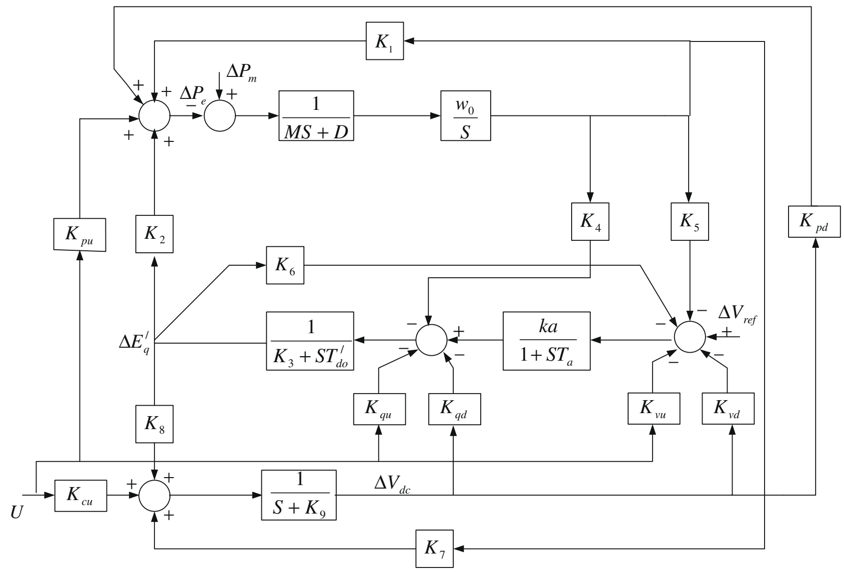

Fig. 3. Modified Heffron–Phillips transfer function model.

$$\dot{x} = A_C x \quad (28)$$

where A_c is the closed-loop state matrix and is given by

$$A_C = A - BKC \quad (29)$$

By properly choosing the feedback gain K, the eigenvalues of closed-loop matrix A_c are moved to the left-hand side of the complex plane and the desired performance of controller can be achieved. The output feedback signals can be selected by using mode observability analysis [22,23]. Once the output feedback signals are selected, only the selected signals are used in forming Eq. (26). Thus, the remaining problem in the design of output feedback controller is the selection of K to achieve the required objectives. The control objective is to increase the damping of the critical modes to the desired level. It should be noted that the four control parameters of the UPFC (m_B, m_E, δ_B and δ_E) can be modulated in order to produce the damping torque. In this paper, δ_E and m_B are modulated in order to damping controller design and are compared with the classical PSS. The proposed controller must be able to work well under all the operating conditions where the improvement in damping of the critical modes is necessary. Since the selection of the output feedback gains for mentioned UPFC based damping controller is a complex optimization problem. Thus, to acquire an optimal combination, this paper employs PSO [26] to improve optimization synthesis and find the global optimum value of objective function. A performance index based on the system dynamics after an impulse disturbance alternately occurs in the system is organized and used to form the objective function of the design problem. In this study, an Integral of Time multiplied Absolute value of the Error (ITAE) is taken as the objective function. Since the operating conditions in power systems are often varied, a performance index for a wide range of operating points is defined as follows:

$$J = \sum_{i=1}^{Np} \int_0^{tsim} t|\Delta\omega_i|dt \quad (30)$$

where t_{sim} is the time range of simulation and N_P is the total number of operating points for which the optimization is carried out. For objective function calculation, the time-domain simulation of the power system model is carried out for the simulation period. It is aimed to minimize this objective function in order to improve the system response in terms of the settling time and overshoots. The design problem can be formulated as the following constrained optimization problem, where the constraints are the controller parameters bounds [25]:

Minimize J subject to:

$$K_1^{\min} \leqslant K_1 \leqslant K_1^{\max}$$
$$K_2^{\min} \leqslant K_2 \leqslant K_2^{\max} \quad (31)$$

Typical ranges of the optimized parameters are [0.01–150] for K_1 and [0.01–10] for K_2. The proposed approach employs PSO algorithm to solve this optimization problem and search for an optimal set of output feedback controller parameters. The optimization of UPFC controller parameters is carried out by evaluating the objective cost function as given in Eq. (31), which considers a multiple of operating conditions. The operating conditions are considered as:

- Base case: P = 0.80 pu, Q = 0.114 pu and X_L = 0.3 pu.
- Case 1: P = 0.2 pu, Q = 0.01 and X_L = 0.3 pu.
- Case 2: P = 1.20 pu, Q = 0.4 and X_L = 0.3 pu.
- Case 3: P = 0.80 pu, Q = 0.114 pu and X_L = 0.6 pu.
- Case 4: P = 1.20 pu, Q = 0.4 and X_L = 0.6 pu.

In this work, in order to acquire better performance, number of particle, particle size, number of iteration, c_1, c_2, and c is chosen as 30, 2, 50, 2, 2 and 1, respectively. Also, the inertia weight, w, is linearly decreasing from 0.9 to 0.4. It should be noted that PSO algorithm is run several times and then optimal set of output feedback gains for the UPFC controllers is selected. The final values of the optimized parameters are given in Table 1.

4. Nonlinear time-domain simulation

To assess the effectiveness and robustness of the proposed controller, simulation studies are carried out for various fault disturbances and fault clearing sequences for two scenarios.

Table 1
The optimal parameter settings of the proposed controllers.

Controller	K_1	K_2
PSS	118.05	0.5112
m_B	115.14	3.127
δ_E	60.18	0.31

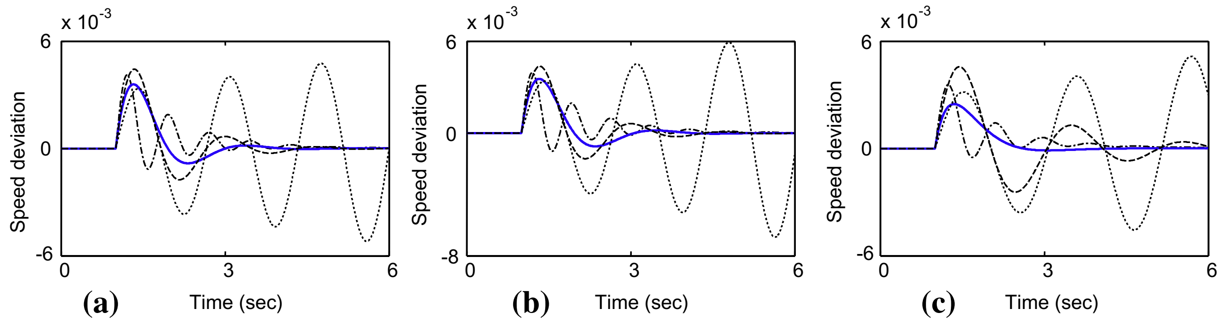

Fig. 4. Dynamic responses for $\Delta\omega$ in scenario 1 at: (a) base case (b) case 2 (c) case 4 loading; solid (δ_E based controller), dashed (m_B based controller), dash-dotted (PSS) and dotted (without controller).

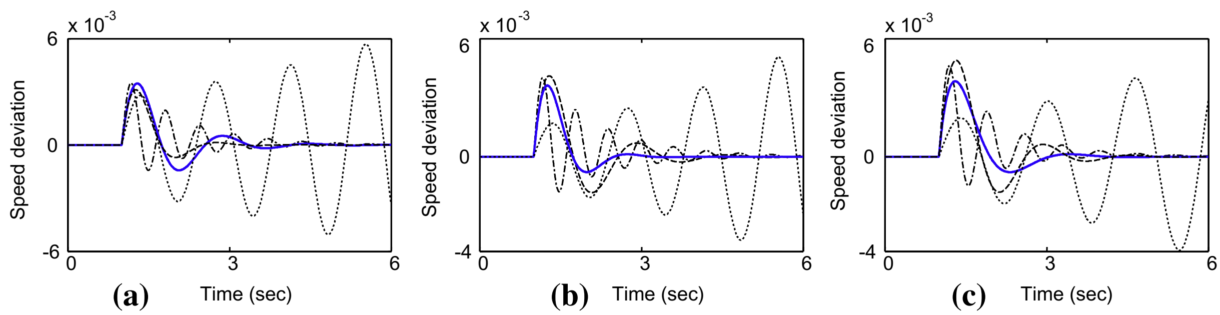

Fig. 5. Dynamic responses for $\Delta\omega$ in scenario 2 at: (a) base case (b) case 2 (c) case 4 loading; solid (δ_E based controller), dashed (m_B based controller), dash-dotted (PSS) and dotted (without controller).

4.1. Scenario 1

In this scenario, the performance of the proposed controller under transient conditions is verified by applying a 6-cycle three-phase fault at $t = 1$ s, at the middle of the one transmission line. The fault is cleared by permanent tripping of the faulted line. The speed deviation of generator at base case, case 2 and case 4 with the proposed controller based on the δ_E, m_B and power system stabilizer (PSS) are shown in Fig. 4. It can be seen that the PSO-based designed controller achieves good robust performance, provides superior damping in comparison with the conventional PSS and enhance greatly the dynamic stability of power systems.

4.2. Scenario 2

In this scenario, another severe disturbance is considered for different loading conditions; that is, a 6-cycle, three-phase fault is applied at the same above mentioned location in scenario 1. The fault is cleared without line tripping and the original system is restored upon the clearance of the fault. The system response to this disturbance is shown in Fig. 5. It is also clear form the figure that the proposed method has good damping characteristics for low frequency oscillations and stabilizes the system quickly.

From the above conducted tests, it can be concluded that the δ_E based controller is superior to the m_B based controller. To demonstrate performance robustness of the proposed method, two performance indices: the ITAE and Figure of Demerit (FD) based on the system performance characteristics are defined as [27]:

$$\begin{aligned} ITAE &= 10{,}000 \int_0^5 t|\Delta\omega|dt \\ FD &= (1000 \times OS)^2 + (4000 \times US)^2 + T_s^2 \end{aligned} \tag{32}$$

where speed deviation ($\Delta\omega$), Overshoot (OS), Undershoot (US) and settling time of speed deviation of the machine is considered for evaluation of the $ITAE$ and FD indices. It is worth mentioning that the lower the value of these indices is, the better the system response in terms of time-domain characteristics. Numerical results of performance robustness for all system loading cases are listed in Table 2. It can be seen that the values of these system performance characteristics with the output feedback δ_E based controller are much smaller compared to output feedback m_B based controller and PSS. This demonstrates that the overshoot, undershoot, settling

Table 2
Values of performance indices *ITAE* and *FD*.

Fault case	Controller	Base case		Case 1		Case 2		Case 3		Case 4	
		ITAE	FD	ITAE	FD	ITAE	FD	ITAE	FD	ITAE	FD
With tripping line	*PSS*	50.25	80.50	94.09	188.73	61.05	79.40	75.02	73.11	83.42	75.62
	m_B	70.89	130.4	90.41	151.62	84.61	122.39	73.34	46.18	63.11	84.48
	δ_E	46.10	37.55	22.41	16.13	48.33	39.01	41.57	21.68	46.15	23.32
Without tripping line	*PSS*	56.44	90.87	92.21	190.06	58.48	96.28	55.55	82.82	56.87	79.43
	m_B	50.35	63.01	42.65	60.32	55.98	70. 32	72.95	108.25	71.71	98.62
	δ_E	49.63	60.44	21.31	22.61	53.75	65.10	33.89	23.41	38.26	29.50

Table 3
System parameters.

Generator	$M = 8$ MJ/MVA	$T'_{do} = 5.044$s	$X_d = 1$ pu
	$X_q = 0.6$ pu	$X'_d = 0.3$ pu	$D = 0$
Excitation system		$K_a = 10$	$T_a = 0.05$ s
Transformers		$X_T = 0.1$ pu	$X_E = 0.1$ pu
		$X_B = 0.1$ pu	
Transmission line		$X_L = 1$ pu	
Operating condition		$P = 0.8$ pu	$V_b = 1.0$ pu
		$V_t = 1.0$ pu	
DC link parameter		$V_{DC} = 2$ pu	$C_{DC} = 1$ pu
UPFC parameter		$m_B = 0.08$	$\delta_B = -78.21°$
		$\delta_E = -85.35°$	$m_E = 0.4$
		$K_s = 1$	$T_s = 0.05$

time and speed deviations of the machine are greatly reduced by applying the proposed control approach. Moreover, it can be concluded that the δ_E based controller is the most robust controller.

5. Conclusions

The particle swarm optimization algorithm has been successfully applied to the design of robust output feedback UPFC based damping controller. The design problem of the robustly selecting output feedback controller parameters is converted into an optimization problem which is solved by a PSO technique with the time domain-based objective function. Only the local and available state variables $\Delta\omega$ and ΔV_t are taken as the input signals of each controller, so the implementation of the designed stabilizers becomes more feasible. The effectiveness of the proposed UPFC controller for improving transient stability performance of a power system are demonstrated by a weakly connected example power system subjected to different severe disturbances under different operating conditions. The nonlinear time-domain simulation results show that the oscillations of synchronous machines can be quickly and effectively damped for power systems with the proposed controller. The system performance characteristics in terms of '*ITAE*' and '*FD*' indices reveal that the output feedback δ_E based damping controller demonstrates its superiority than both output feedback m_B based controller and *PSS* at various fault disturbances and fault clearing sequences.

Appendix A

The nominal parameters and operating condition of the system are listed in Table 3.

References

[1] Al-Awami AT, Abdel-Magid YL, Abido MA. A particle-swarm-based approach of power system stability enhancement with unified power flow controller. Elect Power Energy Syst 2007;29:251–9.
[2] Anderson PM, Fouad AA. Power system control and stability. Ames, IA: Iowa State Univ. Press; 1977.
[3] Keri AJF, Lombard X, Edris AA. Unified power flow controller: modeling and analysis. IEEE Trans Power Deliver 1999;14(2):648–54.
[4] Tambey N, Kothari M. Unified power flow controller based damping controllers for damping low frequency oscillations in a power system; 2003. <http://www.ieindia.org/publish/el/0603>.
[5] Gyugyi L. Unified power-flow control concept for flexible ac transmission systems. IEE Proc Gen Transm Dist 1992;139(4):323–31.
[6] Hingorani NG, Gyugyi L. Understanding FACTS: concepts and technology of flexible AC transmission systems. Wiley IEEE Press; 1999.
[7] Vilathgamuwa M, Zhu X, Choi SS. A robust control method to improve the performance of a unified power flow controller. Elect Power Syst Res 2000;55:103–11.
[8] Song YH, Johns AT. Flexible ac transmission systems (FACTS). UK: IEE Press; 1999.
[9] Nabavi-Niaki A, Iravani MR. Steady-state and dynamic models of unified power flow controller (UPFC) for power system studies. IEEE Trans Power Syst 1996;11(4):1937–43.
[10] Wang HF. A unified model for the analysis of FACTS devices in damping power system oscillations – part III: unified power flow controller. IEEE Trans Power Deliver 2000;15(3):978–83.
[11] Wang HF. Damping function of unified power flow controller. IEE Proc Gen Transm Dist 1999;146(1):81–7.
[12] Wang HF. Application of modeling UPFC into multi-machine power systems. IEE Proc Gen Transm Dist 1999;146(3):306–12.
[13] Wang HF, Swift FJ. A Unified model for the analysis of FACTS devices in damping power system oscillations part I: single-machine infinite-bus power systems. IEEE Trans Power Deliver 1997;12:941–6.
[14] Huang Z, Ni Y, et al. Control strategy and case study. IEEE Trans Power Syst 2000;15(2):817–24.
[15] Dash PK, Mishra S, Panda G. A radial basis function neural network controller for UPFC. IEEE Trans Power Syst 2000;15(4):1293–9.
[16] Pal BC. Robust damping of interarea oscillations with unified power flow controller. IEE Proc Gen Transm Dist 2002;149(6):733–8.
[17] Kazemi A, Vakili Sohrforouzani M. Power system damping controlled facts devices. Elect Power Energy Syst 2006;28:349–57.
[18] Dash PK, Mishra S, Panda G. Damping multimodal power system oscillation using hybrid fuzzy controller for series connected FACTS devices. IEEE Trans Power Syst 2000;15(4):1360–6.
[19] Limyingcharone S, Annakkage UD, Pahalawaththa NC. Fuzzy logic based unified power flow controllers for transient stability improvement. IEE Proc Gen Transm Dist 1998;145(3):225–32.
[20] Khon L, Lo KL. Hybrid micro-GA based FLCs for TCSC and UPFC in a multi machine environment. Elect Power Syst Res 2006;76:832–43.
[21] Mok TK, Liu H, Ni Y, Wu FF, Hui R. Tuning the fuzzy damping controller for UPFC through genetic algorithm with comparison to the gradient descent training. Elect Power Energy Syst 2005;27:275–83.
[22] Chen XR, Pahalawaththa NC, Annakkage UD, Cumble CS. Design of decentralized output feedback TCSC damping controllers by using simulated annealing. IEE Proc Gen Transm Dist 1998;145(5):553–8.
[23] Chen XR, Pahalawaththa NC, Annakkage UD, Cumble CS. Output feedback TCSC controllers to improve damping of meshed multimachine power systems. IEE Proc Gen Transm Dist 1997;144(3):243–8.
[24] Shayeghi H, Jalili A, Shayanfar HA. Multi-stage fuzzy load frequency control using PSO. Energy Convers Manage 2008;49:2570–80.
[25] Kennedy J, Eberhart R, Shi Y. Swarm intelligence. San Francisco: Morgan Kaufman Publishers; 2001.
[26] Clerc M, Kennedy J. The particle swarm-explosion, stability, and convergence in a multidimensional complex space. IEEE Trans Evolut Comput 2002;6(1):58–73.
[27] Shayeghi H, Shayanfar HA, Jalili A. Multi stage fuzzy PID power system automatic generation controller in deregulated environments. Energy Convers Manage 2006;47:2829–45.
[28] Lee S. Optimal decentralized design for output-feedback power system stabilizers. IEE Proc Gen Transm Dist 2005;152(4):494–502.

Hossein Shayeghi received the B.S. and M.S.E. degrees in Electrical Engineering from KNT and Amirkabir Universities of Technology in 1996 and 1998, respectively and the PhD degree in Electrical Engineering from Iran University of Science and Technology (IUST), Tehran, Iran, in 2006. Currently, he is an Assistant Professor at Technical Engineering Department of University of Mohaghegh Ardabili, Ardabil, Iran. His research interests are in the application of Robust Control, FACTS Devices, Artificial Intelligence to load forecasting, power system control design, planning and power system restructuring. He is a member of Iranian Association of Electrical and Electronic Engineers (IAEEE) and IEEE.

Heidarali Shayanfar received the B.S. and M.S.E. degrees in Electrical Engineering in 1973 and 1979, respectively. He received his PhD degree at Electrical Engineering from Michigan State University, U.S.A., in 1981. Currently, he is a Full Professor in Electrical Engineering Department of Iran University of Science and Technology, Tehran, Iran. His research interests are in the Application of Artificial Intelligence to power system control design, Dynamic Load Modeling, Power System Observability

studies and Voltage Collapse. He is a member of Iranian Association of Electrical and Electronic Engineers and IEEE.

Saieed Jalilizadeh received the PhD degree in Electrical Engineering from Iran University of Science and Technology (IUST), Tehran, Iran, in 2006. Currently, he is an Assistant Professor at Technical Engineering Department of Zanjan University, Zanjan, Iran. His research interests are power system contingency analysis and power system planning.

Amin Safari is a M.S. student in Electrical Engineering at the Zanjan University, Zanjan, Iran. His areas of interest in research are application of FACTS Devices and Artificial Intelligence based optimization technique to power system control.